Modeling of Bearingless Permanent Magnet Synchronous Motor Based on Mechanical to Electrical Coordinates Transformation

Ying Xu [1], Huangqiu Zhu, Mengyao Wu

[1] School of Electrical and Information Engineering, Jiangsu University, China, Zhenjiang, 15751001067@163.com

***Abstract*—A bearingless permanent magnet synchronous motor(BPMSM) has two sets of stator windings, namely torque windings and suspension force windings, so there are two types of air-gap magnetic fields, torque windings' and suspension force windings', with different pole-pair in the motor. The analysis of the flux linkage intersection between the two sets of the windings is the foundation of setting up the precise mathematical model of the motor. By the application of mechanical-to-electrical coordinate transformation, this paper refers to a detailed analysis of the flux linkage intersection between torque windings and suspension force windings. And it has been proved that if the pole-pair of torque windings and suspension force windings are P_M=1 and P_B=2, respectively (or P_B=1, P_M=2), flux linkage of the torque windings and suspension force windings will be mutual coupling. The whole proof is simple, objective and easy to understand with a clear concept. What's more, based on the conclusions proved above, the general mathematical model of BPMSM is set up. Finally, the experiment results have shown that the established mathematical model is feasible and accurate.**

I. INTRODUCTION

A Bearingless permanent magnet synchronous motor (BPMSM) is a new type of machine combining the excellent characteristics of conventional permanent magnet synchronous motor (PMSM) and magnetic bearings[1-2]. Therefore, it has some excellent performances of a PMSM, such as great power density, high power factor and high efficiency, as well as obtains some excellent characteristics of magnetic bearings, such as no mechanical friction, no lubrication, no pollution, long life-span and little maintenance. Combined with all the merits, the motor can realize bearingless technology and run at a high or ultra-high speed. In recent years, with the development of digital signal processing technology, power electronic technology, and modern control theory, research on BPMSM has made much progress. Furthermore, with ever-increasing application potentials in centrifugal machines, turbo molecular pumps, high-speed-precision mechanical processing, aeronautics and astronautics, flywheel energy storage, and life science, there is a fast growing interest in BPMSM [3-6].

There are two types of air-gap magnetic fields, torque windings' and suspension force windings', with different pole-pairs in the motor. Therefore, the analysis of the flux linkage intersection between the two sets of the windings is the foundation of establishing the accurate mathematical model. Literature [7] has proposed a method to obtain the flux linkage equations between torque windings and suspension force windings through experiments. A mathematical expression of electromagnetic energy was derived, and the mathematical expressions were then derived through differential. The method taking advantage of the virtual displacement principle to solve radial forces is convenient in the field of deriving the mathematical expressions of radial forces in a bearingless motor, but the error caused by experiment measurement is rather larger. In literature [8], not only were the method of differential of electromagnetic energy to derive radial forces and electromagnetic torque given, but also the general formula of radial forces and electromagnetic torque were derived by the integral method. At present, differential and integral methods are the most essential methods for deducing mathematical expressions of radial suspension forces for the bearingless motors, but the concept is not easy to visualized and difficult to understand. In literature [9], a method of transforming mechanical coordinates to electrical coordinates was put forward. Based on the method, the mathematical model of BPMSM was set up with the characteristics of simpleness, clear concept, easy understanding, etc.. But the established mathematical model was only for the pole-pairs of torque windings and suspension force windings P_M=2, P_B=3, respectively, detailed analysis of the scope of application of the model was not given, and the flux linkage intersection between the two sets of the windings was not analyzed.

The objective of this paper is to give a detailed analysis of the flux linkage intersection between torque windings and suspension force windings through the application of mechanical-to-electrical coordinate transformation. And, it has been proved that if the pole-pairs of torque windings and suspension force windings are P_M=1, P_B=2, respectively (or P_B=1, P_M=2), flux linkage of the torque windings and suspension force windings will be mutual coupling. Based on the flux linkage intersection, flux linkage equations and voltage equations of torque windings and suspension force windings are obtained. After analyzing the influence of every Lorentz force on electromagnetic torque in the BPMSM, the equation of electromagnetic torque of the BPMSM is derived. Then, according to the characteristic and structure of the coefficient in the equations of radial forces, the complete mathematical expressions of radial forces are given. At last, a control diagram for the BPMSM experiment system is introduced, and the experiment waves are given.

II. The Structure and Suspension Principle of BPMSM

A. Mechanical Structure of BPMSM

The 2-degree-of-freedom(DOF) BPMSM is applied as a research object in this paper, the structure is shown in Fig. 1. An incremental photoelectric coded disk is installed on the end cap, to measure the rotor speed and rotation angle of the motor in real time. And, the sensors connected to an eddy current sensor probe is used to measure the radial displacement of the rotor in real time. At the right end of the shaft, an auxiliary bearing is equipped to support the rotor when the motor is in a stationary state.

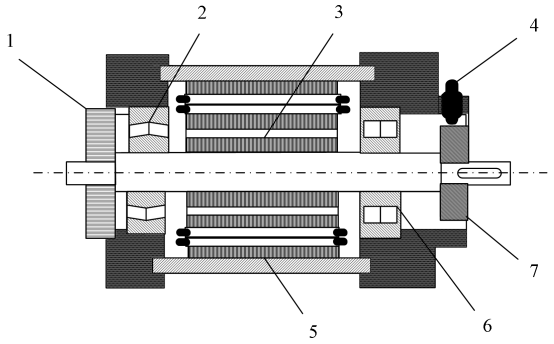

Figure. 1. Internal mechanical structure of BPMSM
1. Photoelectrical encoder 2. Self-aligning ball bearing 3. Rotor 4. Position sensor probe 5. Stator 6. Auxiliary bearing 7. Benchmark ring

B. Suspension Principle of BPMSM

The essence of the radial suspension force of the bearingless motor is that the magnetic field generated by the suspension force winding breaks the balance of the air gap magnetic field established by the original torque winding, and thus the radial suspension force acting on the rotor side is generated. Assume the pole-pair number of torque windings is P_M and the pole-pair number of suspension force windings is P_B, through the theory and practice proved: the rotating magnetic field generated by energizing the suspension force winding and the magnetic field generated by the torque winding satisfy: a) $P_B=P_M \pm 1$; b) the two magnetic fields have the same direction of rotation; c) when the current frequency which generates the magnetic field is the same , the combined magnetic field generated by the two magnetic fields interacts to stabilize the rotor of the motor.

If $P_M=1$ and $P_B=2$, the forces acting on the surface of the rotor can be seen in Fig. 2, in which the big windings are torque windings, and the small ones are suspension force windings. As shown in Fig. 2(a), the forces named Maxwell forces are marked on the surface of the rotor. And, the direction of Maxwell force is vertical upwards and the rotor is acted by radial force in the vertical upwards direction, as depicted in the same figure. In Fig. 2(b), according to the left-hand rule, the torque windings and the suspension windings are subjected Lorentz forces, whose directions are shown in the stator. Furthermore, based on Newton's third law of motion, opposite forces appear in the rotor. It can be seen that the direction of these two different resultant forces are opposite, the direction of total resultant force is upward, so the rotor is acted by a radial force with the upward direction. According to the analysis above, it can be concluded that Maxwell forces and Lorentz forces are the two main radial forces making the rotor suspend steadily in the bearingless motor.

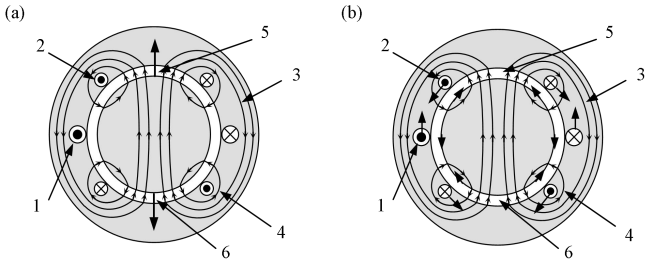

(a) Maxwell force (b) Lorentz force

Figure. 2. Sketches of forces on motor's rotor in unbalanced magnetic field 1. Torque windings 2. Suspension force windings 3. Torque windings' flux 4. Suspension force windings' flux 5. Enhanced point of the magnetic field 6. Weak point of the magnetic filed

III. Analysis of the Flux Linkage Intersection Between the Two Sets of the Windings in BPMSM.

A. Variable definitions between two sets of windings in BPMSM

The concept of mechanical-to-electrical coordinate transformation is introduced in this part. Two-phase rotating coordinate system established in a mechanical angle cycle is called "mechanical coordinate system" (shown in Fig. 3(a) *doq*, Fig. 4(a) *doq*). Likewise, two-phase rotating coordinate system established in a electrical angle cycle is called "electrical coordinate system" (shown in Fig. 3(d) d_1oq_1, Fig. 4(d) d_1oq_1). The process of transforming a mechanical coordinate system into a number of electrical coordinate systems is referred to as "mechanical-to-electrical coordinate transformation". Based on the application of "mechanical-to-electrical coordinate transformation" method, then, this paper refers to do a detailed analysis of the flux linkage intersection between the two sets of the windings.

Supposing that turning counterclockwise is the positive direction, and the rotor rotates in the positive direction with mechanical angular velocity ω. Thus, the rotating electrical angular velocity of the torque windings air-gap magnetic fields will be $P_M\omega$. So will be the rotating electrical angular velocity of the suspension force windings air-gap magnetic filed. Further, both of the air-gap magnetic fields rotate in the positive direction. In order to analyze the flux linkage interaction relations between the two sets of the windings in detail, the definition of some related concepts are listed in Table I. As the experiment platform adopted is a surface-mounted BPMSM, for suspension force windings, $L_{Bd}=L_{Bq}=L_B$, and for torque windings, $L_{Md}=L_{Mq}=L_M$. Where L_B and L_M are the self-inductance of suspension force windings and torque windings, respectively. L_{Bd} and L_{Bq} are the *d*-axis and *q-axis* self-inductance of suspension force windings, respectively, L_{Md} and L_{Mq} are the corresponding terms of the torque windings.

TABLE I. THE DEFINITION OF SOME RELATED CONCEPTS

Symbols	Definition
Ψ_B	the air-gap flux linkage produced by suspension force windings
Ψ_M	the air-gap flux linkage produced by torque windings
Ψ_{PM}	the air-gap flux linkage produced by permanent magnet
Ψ_{Bd} Ψ_{Bq}	the d-axis component and q-axis component of Ψ_B
Ψ_{Md} Ψ_{Mq}	the d-axis component and q-axis component of Ψ_M
i_B	the current amplitude of the suspension force windings in the two-phase rotating coordinates
i_M	the current amplitude of the torque windings in the two-phase rotating coordinates
i_{Bd} i_{Bq}	the d-axis component and q-axis component of i_B
i_{Md} i_{Mq}	the d-axis component and q-axis component of i_M

B. Analysis of the flux linkage intersection between the two sets of the windings in BPMSM

When the pole-pairs of torque windings and suspension force windings are P_M=1, P_B=2, respectively, the mechanical coordinate system of torque windings in the BPMSM is shown in Fig. 3 (a). And the two-phase rotating coordinate system of suspension force windings are shown in Fig. 3 (b) and Fig. 3 (c), under which a equation set can be expressed as:

$$\begin{cases} i_{Bd} = i_B \cos(\theta_B) \\ i_{Bq} = i_B \sin(\theta_B) \\ \psi_B = L_B i_B \\ \psi_{Bd} = \psi_B \cos(\theta_B) = L_B i_B \cos(\theta_B) = L_B i_{Bd} \\ \psi_{Bq} = \psi_B \sin(\theta_B) = L_B i_B \sin(\theta_B) = L_B i_{Bq} \end{cases} \quad (1)$$

In Fig. 3(a), θ is a rotary angle between air-gap magnetic fields of suspension force windings and torque windings. As the mechanical angular velocity between air-gap magnetic fields of torque windings and suspension force windings is $\omega/2-\omega=-\omega/2$, the value of θ will be negative.

The electrical coordinate system shown in Fig. 3(d) is obtained through the method of transforming mechanical coordinate system in Fig. 3(a). As indicated in Fig. 3(d), the *d*-axis component and *q*-axis component of Ψ_B are described as:

$$\begin{cases} \psi_B \cos(P_M\theta) - \psi_B \cos(P_M\theta) = 0 \\ \psi_B \sin(P_M\theta) - \psi_B \sin(P_M\theta) = 0 \end{cases} \quad (2)$$

Consequently, the equation of the flux linkage generated by torque windings can be written as:

$$\begin{cases} \psi_{Md} = L_M i_{Md} + \psi_{PM} \\ \psi_{Mq} = L_M i_{Mq} \end{cases} \quad (3)$$

It can be seen that i_{Md} and i_{Mq} are depicted in Fig. 4(b), where $i_{Md}=i_M \cos(\theta_M)$ and $i_{Mq}=i_M \sin(\theta_M)$.

The mechanical coordinate system of suspension force windings in the BPMSM is shown in Fig. 4(a). And the two-phase rotating coordinate systems of torque windings are shown in Fig. 4(b) and Fig. 4(c), under which equations can be given by:

$$\begin{cases} i_{Md} = i_M \cos(\theta_M) \\ i_{Mq} = i_M \sin(\theta_M) \\ \psi_M = L_M i_M \\ \psi_{Md} = \psi_M \cos(\theta_M) = L_M i_M \cos(\theta_M) = L_M i_{Md} \\ \psi_{Mq} = \psi_M \sin(\theta_M) = L_M i_M \sin(\theta_M) = L_M i_{Mq} \end{cases} \quad (4)$$

If the value of θ_M is zero, θ shown in Fig. 4(a) will be the rotary angle of air-gap magnetic filed generated by torque windings relative to air-gap magnetic filed produced by suspension force windings. (corresponding to Fig. 3(a), at this moment θ is positive). The first electrical coordinate system of suspension force windings shown in Fig. 4(d) is obtained from Fig. 4(a) by the application of mechanical-to-electrical coordinate transformation. As seen from Fig. 4(d), the d-axis and q-axis components of Ψ_M are $\Psi_M \cos(P_B\theta)$ and $\Psi_M \cos(P_B\theta)$. As can be seen from Fig. 4(a), Ψ_M and its components disappear in the second electrical coordinate system. From the analysis above, the equation of the flux linkage generated by suspension force windings can be given by:

$$\begin{cases} \psi_{Bd} = L_B i_{Bd} + \psi_M \cos(P_B\theta) \\ \psi_{Bq} = L_B i_{Bq} + \psi_M \sin(P_B\theta) \end{cases} \quad (5)$$

From (3) and (5), it can be seen that when the pole-pairs of torque windings and suspension force windings are P_M=1, P_B=2, respectively, the flux linkage of torque windings is not affected by suspension force windings, but the flux linkage of suspension force windings is influenced by torque windings. Similarly, through the analysis of the same method we can draw the conclusion that if the pole-pairs of torque windings and suspension force windings are P_M=2, P_B=1, respectively, the flux linkage of torque windings will be affected by suspension force windings, but the flux linkage of suspension force windings will not be influenced by torque windings. May know by above, if the pole-pairs of torque windings and suspension force windings are P_M=1, P_B=2, respectively (or P_B=1, P_M=2), flux linkage of the torque windings and suspension force windings will be mutual coupling.

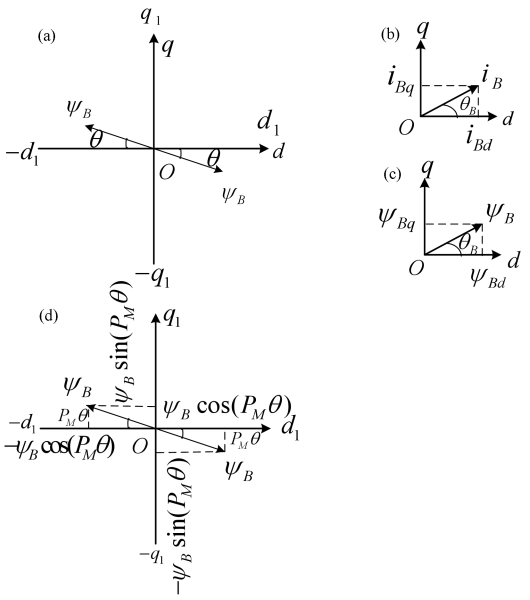

Figure. 3. Sketches of mechanical to electrical coordinate transformation in torque windings of BPMSM

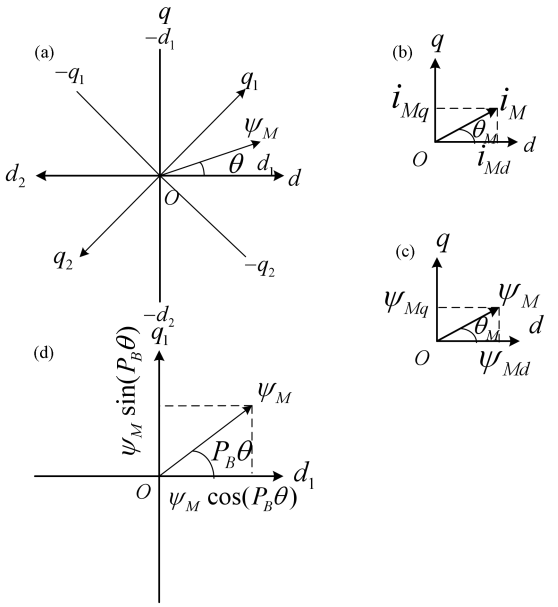

Figure. 4. Sketches of mechanical to electrical coordinate transformation in suspension force windings of BPMSM

IV. Modeling Based on Mechanical to Electrical Coordinate Transformation

A. Flux linkage equations in BPMSM

A BPMSM has two main functions, generating electromagnetic torque and radial forces. Therefore, the mathematical model of BPMSM should include six main equations: flux linkage equations of suspension force windings, flux linkage equations of torque windings, voltage equations of suspension force windings, voltage equations of torque windings, electromagnetic torque of BPMSM, and radial suspension force windings. Known from the analysis of the above, if the flux linkage intersection between the two sets of the windings under the situation that the pole-pairs of torque windings and suspension force windings are P_M=1, P_B=2 respectively, the flux linkage equations of torque windings and suspension force windings will be expressed as follows:

$$\begin{cases} \psi_{Md} = L_M i_{Md} + \psi_{PM} \\ \psi_{Mq} = L_M i_{Mq} \end{cases} \tag{6}$$

$$\begin{cases} \psi_{Bd} = L_B i_{Bd} + \psi_M \cos(P_B\theta) \\ \psi_{Bq} = L_B i_{Bq} + \psi_M \sin(P_B\theta) \end{cases} \tag{7}$$

B. Voltage equations in BPMSM

Constant load, stable rotating velocity and rotor steadily suspending without magnetic flux control all these three conditions are satisfied, in other words, i_{Md}, i_{Mq} and ψ_{PM} are constant in eq. (6), so the voltage equations of torque windings can be given by:

$$\begin{cases} u_{Md} = -P_M \omega \psi_{Mq} + R_M i_{Md} \\ u_{Mq} = P_M \omega \psi_{Md} + R_M i_{Mq} \end{cases} \tag{8}$$

Where R_M is the resistance of torque windings in the two-phase rotating coordinate.

Under the condition of the rotor suspending steadily, the voltage equations of suspension force windings can be written as:

$$\begin{cases} u_{Bd} = -P_M \omega \psi_{Bq} + R_B i_{Bd} \\ u_{Bq} = P_M \omega \psi_{Bd} + R_B i_{Bq} \end{cases} \tag{9}$$

Where R_B is the resistance of suspension force windings in the two-phase rotating coordinate.

C. Electromagnetic torque and radial suspension force equations in BPMSM

If the rotor is in the center position, the mathematical expression of electromagnetic torque of the BPMSM will be the same as that of the general PMSM [10].

$$T_{em} = P_M \psi_{PM} i_{Mq} \tag{10}$$

As described in literature [9], the radial suspension force equation of the BPMSM can be written into:

$$\begin{bmatrix} F_x \\ F_y \end{bmatrix} = k_m \sqrt{\left(I_{PM} + i_{Md}\right)^2 + i_{Mq}^2} \cdot \begin{bmatrix} i_{Bd} \\ i_{Bq} \end{bmatrix} + k_c \left[\left(i_{PM} + i_{Md}\right)^2 + \left(k_q i_{Mq}\right)^2 \right] \cdot \begin{bmatrix} x \\ y \end{bmatrix} \tag{11}$$

Where k_m, k_c and k_q are all constant, i_{PM} is the equivalent current component in torque windings caused by magnetic filed produced by permanent magnet of the rotor, x, y are the displacement in x, y direction.

V. Simulation Analyses and Experimental Results

A. Simulation analyses in BPMSM

A control algorithm, which is on the basis of rotor magnetic field oriented control strategy, is adopted in the BPMSM and the vector control system block diagram is shown in Fig. 5. Thus, closed-loop control of rotational speed and radial suspension force are achieved by detecting rotor displacement and three-phase currents. Furthermore, Matlab/simulink is used to simulate the mathematical model of the BPMSM.

Under radial suspension force, the radial displacements of the BPMSM in the *x*- and *y*-direction are shown in Fig. 6 and Fig. 7, and the trajectory of the rotor is shown in Fig. 8. It can be seen from the figures that the rotor can finally achieve stable suspension.

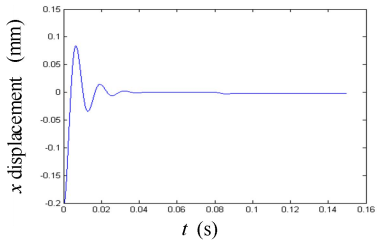

Figure. 6. Radial displacement in the *x* direction

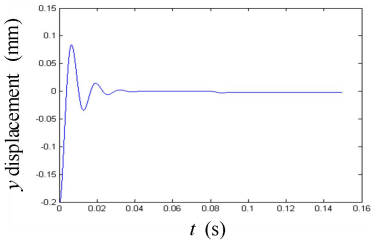

Figure. 7. Radial displacement in the *y* direction

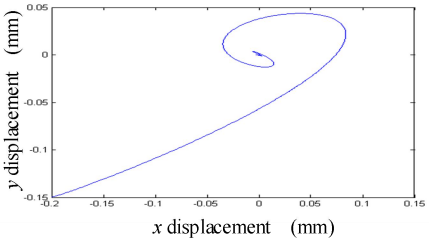

Figure. 8. The diagram of rotor trajectory

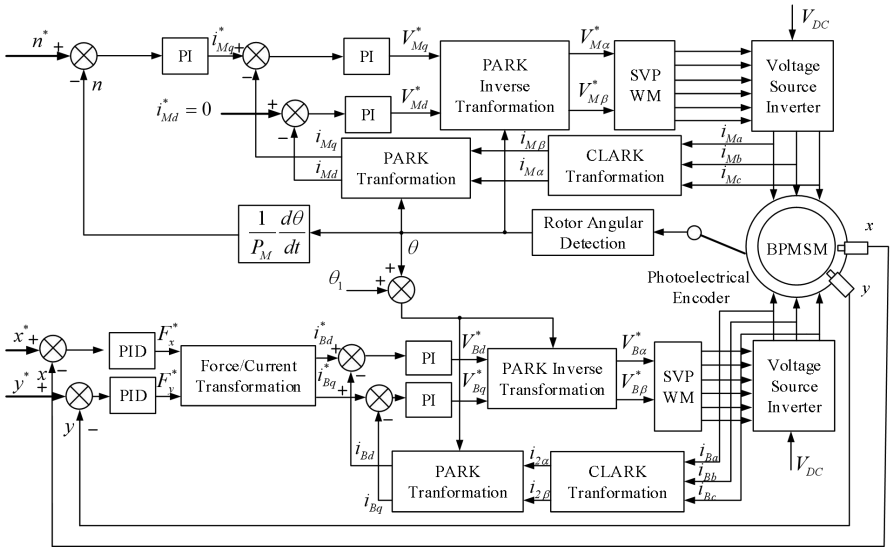

Figure. 5. The digital control block diagram of BPMSM

B. Experimental results of BPMSM

To verify the validity of the proposed analysis method, relevant experiments shown in Fig. 9. are designed and conducted for the 2-DOF BPMSM.

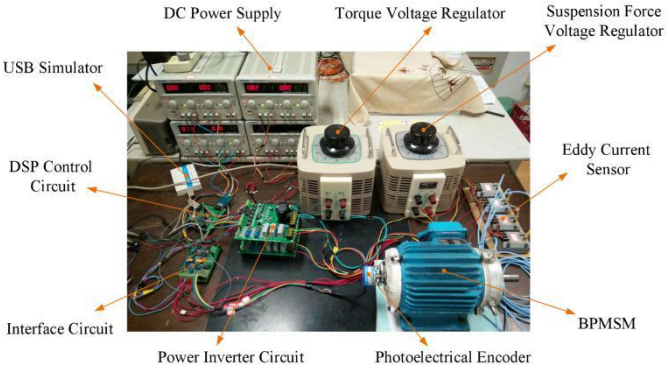

Figure. 9. Digital control platform of the BPMSM

The basic parameters of the experimental prototype are as follows: rated power P_N is 1.1 kW, air gap length g is 1 mm, air gap length $g1$ with the auxiliary bearing is 0.3 mm, rotor outer diameter d_{ro} is 73 mm, permanent magnet thickness h_m is 2 mm, pole-pair of torque windings is 2, torque winding resistance is 2.07 Ω, the *d*- and *q*-axis inductance of the torque windings are 8 mH, pole-pair of suspension force windings is 1, suspension force winding resistance is 1.03 Ω, the *d*-axis and *q*-axis inductance of the suspension force windings are 3.6 mH, the mutual inductance between torque and suspension force windings is 0.16 mH.

From Fig. 10 and Fig. 11, it can be seen that the motor can operate stably at the speed of 3000 r/min, and the generated radial suspension force can limit the rotor to a reciprocating motion near the center position, and the vibration amplitude of the rotor center is 15 μm. Adjusting the parameters of the PID controller will further reduce the amplitude of the motion and ultimately achieve stable suspension of the rotor.

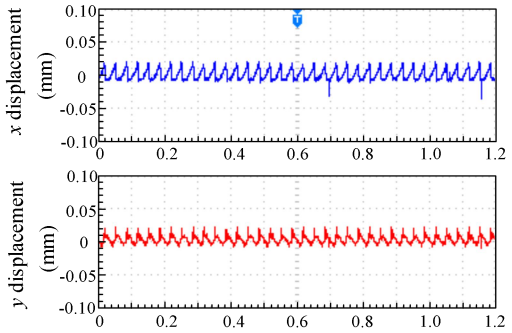

Figure. 10. The radial displacements in the *x*- and *y*-direction when the rotating speed is 3000r/min

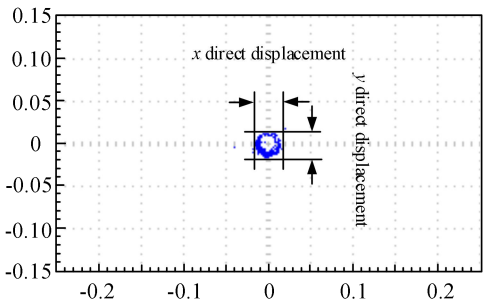

Figure. 11. The orbit of mass center when the rotating speed is 3000r/min

VI. CONCLUSIONS

Based on the application of mechanical-to-electrical coordinate transformation, this paper has demonstrated that if the pole-pairs of torque windings and suspension force windings are P_M=1, P_B=2, respectively (or P_B=1, P_M=2), flux linkage of the torque windings and suspension force windings will be mutual coupling. Based on the basis of proposed concept, the flux linkage equations and voltage equations of torque windings and suspension force windings are given. After analyzing the generated status and function of every Lorentz force, the composing elements of electromagnetic torque of BPMSM is pointed out, and the mathematical expression of electromagnetic torque is deduced. Through analyzing all coefficients in the expression of radial force, the complete equation of radial suspension force is given, and the vector control block diagram and some experiment results are given. The proposed mathematical model of BPMSM in the paper lays the theoretical foundation for simulation study, experiment wave analyses, structural design and improvement of BPMSM.

REFERENCES

[1] X. Sun, L. Chen, and Z. Yang, "Overview of bearingless permanent-magnet synchronous motor," *IEEE Trans. Ind. Electron*., vol. 60, no. 12, pp. 5528-5538, Dec. 2013.

[2] Y. Ren and J. Fang, "Current-sensing resistor design to include current derivative in PWM H-bridge unipolar switching power amplifiers for magnetic bearings," *IEEE Trans. Ind. Electron*., vol. 59, no. 12, pp. 4590-4600, Dec. 2012.

[3] J. Fang and Y. Ren, "Self-adaptive phase-lead compensation based on unsymmetrical current sampling resistance network for magnetic bearing switching power amplifiers, " *IEEE Trans. Ind. Electron*., vol. 59, no. 2, pp. 1218-1227, Feb. 2012.

[4] T. Schuhmann, W. Hofmann, and R. Werner, "Improving operational performance of active magnetic bearings using Kalman filter and state feedback control control," *IEEE Trans. Ind. Electron*., vol. 59, no. 2, pp. 821-829, Feb. 2012.

[5] N. Miyamoto, T. Enomoto, and M. Amada, "Suspension characteristics measurement of a bearingless motor," *IEEE Trans. Magn.,* vol. 45, no. 6, pp. 2795-2798, June. 2009.

[6] J. Asama, M. Amada, and N, Tanabe, "Evaluation of a Bearingless PM Motor with Wide Magnetic Gaps," *IEEE. Trans. Energy Convers*., vol. 25, no. 4, pp. 957-964, Dec. 2010.

[7] A. Chiba, D. T. Power, M. A. Rahman, "Characteristics of a bearingless induction motor," *IEEE Trans. Magn.,* vol. 27, no. 6, pp. 5199-5201, Nov. 1991.

[8] W. Amrhein, S. Silber, K, Nenninger, "Levitation forces in bearingless permanent magnet motors," *IEEE Trans. Magn.,* vol. 35, no. 5, pp. 4052-4054, Sep. 1999.

[9] Q. Cheng, "Control and experiment for bearingless PMSMS," M.S. thesis, Jiangsu Univ., Zhenjiang, China, 2008.

[10] Y. He, H. Nian, B. Luan, "Optimized air-gap-flux orientated control of an induction-type bearingless motor," *Proc. CSEE*., vol. 24, no. 6, pp. 116-121, Jun. 2004.